#3440

NUMERICAL SIMULATION OF THE PERFORMANCE OF BUILDING VENTILATION SYSTEMS

Jin B. Fang
Richard A. Grot
Center for Building Technology
Nation Institute of Standards and Technology
Gaithersburg, MD 20899
USA

ABSTRACT

Mathematical modeling is performed for three-dimensional turbulent buoyant flows emerging from an air diffuser in an air-conditioned, ventilated room subject to diverse supply air velocities. The velocity and temperature distributions of air in the room are calculated, and the calculated results are found to be in reasonable agreement with published experimental observations. Calculations of Air Diffusion Performance Index (ADPI) for a sidewall grille and a return air grille in a room with specified heating loads are carried out for different flow rates of air supply. The predicted ADPI values are found generally to be consistent with the corresponding experimental values. It is reasonable to apply the numerical modeling technique for practical use in the prediction of various air-conditioned room environments and the design of building ventilation systems.

Keywords: air diffusion performance,K-E turbulence models, mathematical modeling, numerical simulation, room air movement ,ventilation systems.

1 Introduction

The comfort level and indoor air quality experienced by occupants in ventilated spaces are dependent on the local air temperature and flow velocity in the occupied zones. Most buiding ventilation systems can provide the desired average temperature and humidity and a certain level of air motion by supplying and removing heat in conditioned spaces. However, there can be areas of excessive air drafts and excessive temperature gradients due to inadequate air distribution and mixing. Similarly, parts of the space may have recirculating or very low air flows, which decrease the effectiveness of ventilation in removing indoor contaminants. The flow behavior and thermal field can also be distorted due to heat and lighting sources, obstacles, ventilation openings and air leakages, and can cause multiple zones of air circulation. For design and selection of a suitable and effective ventilation systems, information on the distribution of air flow velocities and temperatures as well as the heating and cooling loads for given conditioned spaces is needed.

Due to rapid development of computer hardware facilities, computational analysis has been gradually recognized as a cost-effective and convenient way of obtaining detailed solutions for fluid flow and heat transfer problems. It can be noted that various experimental techniques such as field tests for measuring local air velocities and temperatures are expensive and time consuming. Numerical simulation can provide a relatively cheap and rapid means for evaluating the performance of the building ventilation systems and assessing the effects of various system variables such as air supply rate and temperature, and the sizes and locations of air diffusers and exhaust registers. In addition to these, numerical modeling can provide the bases for prediction of thermal comfort and air contaminant dispersion in ventilated spaces with given sources of emission.

The performance of air ventilation systems is dependent on the type of air diffuser used as an air inlet, the space heating or cooling load, and the flow rate of air supply to the conditioned spaces. A properly designed, wall or ceiling mounted air diffuser system can not only meet the required heating and cooling loads but also provide comfort thermal conditions and satisfactory air movement to remove indoor contaminants in the occupied zones.

A comprehensive study of room air distribution performance was conducted by Miller and Nevins [1-4]. They performed extensive laboratory testing of various types of air distribution devices such as sidewall grilles and ceiling diffusers, and evaluated their performances based on the measured air velocities and temperatures in the occupied zone of the test room. Hart and Int-Hout [5] carried out a series of laboratory tests to determine the performance of continuous linear air diffusers in the perimeter zones of both open and closed office configurations. The results of their tests suggest that ceiling mounted linear diffusers can give acceptable thermal environments for a variety of heat loads without the use of convective heaters. Yamazaki, et al. [6] applied numerical modeling technique to simulate the air-heating environments for both a console type of air heater placed in a residential room and an air diffuser installed on the ceiling, and compared the predicted results with some experimental data. Recently, Chen, et al. [7] performed experimental measurements and numerical simulations of air movement, temperature field, and contaminant distributions in a ventilated room under different ventilation rates and heating loads. They have found that numerical predictions generally agree with the measured results, and both the temperature and ventilation efficiencies increase with an increase in ventilation rate.

In this paper, an attempt is made to calculate air flow and thermal fields under the air-conditioned environments using mathematical modeling techniques for a sidewall grille mounted on a wall and directly above the return air outlet in a room of an office building. The predicted results on the air distribution performance of this air diffuser are compared with the published test results [1-4].

2 Calculation Procedure

A finite difference computer program called EXACT3 [8], which stands for EXplicit Algorithm for 3-dimensional Continuous Turbulent fluid flow, was modified with the addition of a source term to the energy equation and used for predicting indoor air movement. This computer code has been used for numerical simulation of indoor air movement and local air contaminant dispersion processes in a chemical laboratory for isothermal flow situation both with and without use of a mechanical ventilation device [9].

The basic equations describing the indoor air flows include the continuity, momentum, and energy equations for a turbulent, buoyancy-affected incompressible fluid, along with two additional transport equations for the turbulence kinetic energy and its dissipation rate, and are expressed by:

$$\frac{\partial U_j}{\partial x_j} = 0 \tag{1}$$

$$\frac{\partial U_i}{\partial t} + \frac{\partial U_i U_j}{\partial x_j} = -\frac{1}{\rho}\frac{\partial P}{\partial x_i} + \frac{\partial}{\partial x_j}\left\{\nu_{eff}\left(\frac{\partial U_i}{\partial x_j} + \frac{\partial U_j}{\partial x_i}\right)\right\} - \beta g_i \theta \tag{2}$$

$$\frac{\partial \theta}{\partial t} + \frac{\partial \theta U_j}{\partial x_j} = \frac{\partial}{\partial x_j}\left(\alpha_{eff}\frac{\partial \theta}{\partial x_j}\right) + S_\theta \tag{3}$$

$$\frac{\partial \kappa}{\partial t} + \frac{\partial \kappa U_j}{\partial x_j} = \frac{\partial}{\partial x_j}\left(\Gamma_\kappa \frac{\partial \kappa}{\partial x_j}\right) + \nu_t S + G - \varepsilon \tag{4}$$

$$\frac{\partial \varepsilon}{\partial t} + \frac{\partial \varepsilon U_j}{\partial x_j} = \frac{\partial}{\partial x_j}\left(\Gamma_\varepsilon \frac{\partial \varepsilon}{\partial x_j}\right) + \frac{\varepsilon}{\kappa}(c_1 \varepsilon \nu_t S - c_2 \varepsilon + c_3 G) \tag{5}$$

where

$\nu_t = C_D \frac{\kappa^2}{\varepsilon}$ eddy viscosity

$\nu_{eff} = \frac{1}{Re} + \nu_t$ effective eddy viscosity

$\alpha_{eff} = \frac{1}{RePr} + \frac{\nu_t}{\sigma_\theta}$ effective thermal diffusivity

$$S = \left(\frac{\partial U_i}{\partial x_j} + \frac{\partial U_j}{\partial x_i} \right) \frac{\partial U_i}{\partial x_j}$$

$$G = \beta g_j \frac{\nu_t}{\sigma_\theta} \frac{\partial \theta}{\partial x_j}$$

$$\Gamma_\kappa = \frac{1}{Re} + \frac{\nu_t}{\sigma_\kappa}$$

$$\Gamma_\varepsilon = \frac{1}{Re} + \frac{\nu_t}{\sigma_\varepsilon}$$

U_i, are mean velocity components in x_i direction, respectively, x_i are Cartesian coordinates, t is time, ρ is the fluid density, P is the pressure, β is the volumetric coefficient of expansion of the fluid, g_j is gravitational acceleration in x_j direction, θ is the temperature difference between the average indoor temperature and local temperature, S_θ is the volumetric rate of heat generation, κ is turbulence kinetic energy, ε is the dissipation rate of turbulence kinetic energy, $Re=L_o U_o/\nu$ is the Reynolds number, in which L_o is the inlet width of air diffuser, U_o is the inlet air velocity , and ν is the kinematic viscosity ; $Pr=\nu/\alpha$ is the Prandtl number, α is the thermal diffusivity of the fluid, and c_1, c_2, c_3, σ_θ, σ_κ and σ_ε are empirical constants in the κ-ε two-equation turbulence model.

Dimensionless variables are introducted into these conservation equations of mass, momentum and energy to give the nondimensional form of the governing equations and the Archimedes number, which is a nondimensional parameter used to characterize the effect of buoyancy on the flow field and defined as $Ar = \beta g_i L_0 \theta_0 / U_0^2$, in which θ_0 is the temperature difference between the supply air and the average room air. These equations are converted into a series of finite difference equations and solved simultaneously by using the MAC method [10]. A staggered grid system is used where the velocity components are defined at the center of grid surface and scalar quantities such as pressure and turbulence kinetic energy are defined at the center of grid volume. The computer code uses a hybrid scheme, which utilizes either centered differencing or upwind differencing schemes depending on the local value of cell Peclet number $Pe = L_0 U_0 / \alpha$, for the partial derivatives in space, and an explicit scheme for the partial derivative with respect to time. It also uses the pressure relaxation technique to correct the pressure and velocity components simultaneously in order to obtain solutions which satisfy the continuity equation. Using the following values for empirical constants appearing in Equations 1 to 5:

$c_D = 0.09$, $c_1 = 1.44$, $c_2 = 1.92$, $c_3 = 1.0$

$\sigma_\kappa = 1.0$, $\sigma_\varepsilon = 1.3$, $\sigma_\theta = 0.9$

and following the MAC method, iterative solving and numerical time integration of these equations were made to obtain the converged solution.

The test room modeled numerically had overall dimensions of 6.10 m wide x 3.66 m long x 2.74 m high, simulating an interior room of a multi-story office building [1-4]. The energy input to the room was composed of electrical and lighting loads. The electrical heat loads were generated by finstrip heaters located around the center of the room floor and having a total heat output of 22.07 W/m^2 over a 3.66 x 1.52 m floor area, and a concentrated load composed of a 0.97 x 0.91 x

0.31 m angle iron framework installed 0.20 m from the south wall, and having a heat output rate of 40.98 W/m^2 of floor area. The ceiling lighting consisted of eight flourescent recessed double-tubed fixtures evenly distributed 0.31 m from the east and west walls and 0.61 m from the end walls of the short dimension and havig a total power input of approximately 760 W. A sidewall grille measuring 0.61 m wide by 0.15 m high was located in the center of the 3.66 m long north wall, with its horizontal center line 0.15 m below the ceiling. A 0.76 m x 0.42 m high return air grille was situated directly beneath the supply air grille, 0.71 m above the floor. Local air temperatures and velocities within the occupied zone of the test room were measured at 216 locations using anemometers and thermocouples. The air supply grilles had two rows of 19 mm wide adjustable vanes and both sets of vanes were straight for all tests performed. For all tests, the room was maintained at an average temperature of 23.33 ± 0.39 C. Under a total heating load of 63.05 W/m^2 of floor area plus a lighting load of 34.09 W/m^2 of floor area, the flow rates of air supply to the room varied from 10.97 to 91.44 m^3/h - m^2 of floor area.

Mathematical modeling was performed to simulate six air distribution tests on the sidewall grille installed in a ventilated room. A numerical grid with the symmetrical half-portion of the room being subdivided non-uniformly into 29 x 27 x 20 rectangular parallelepiped cells was used with six different air flow rates including 10.97, 18.29, 36.58, 54.86, 73.15 and 91.44 m^3/h-m^2 of floor area. In order to deal with boundary conditions, one or two dummy cells with the same cell intervals as that of the terminal real cell were added to outside of the boundary. The temperature difference between the supply air and the average room air for each flow rate was calculated based on an overall energy balance for the whole room. The calculated values of temperature difference between the room air and the supply air, for different rates of air inflow are tabulated in Table 1 along with the Reynolds number and the Archimedes number.

The incoming air was colder than the bulk air in the room to compensate for the input of the room heating loads, simulating a cooling situation. Numerical modeling corresponding to the test conditions was made with a nonuniform mesh layout for a symmetric half portion of the flow domain including the concentrated and uniform heating loads and lighting loads, and an inlet and an outlet opening. Fine grid spacing was used in the vicinity of the walls, the heating loads, and the inlet and outlet openings.

The sidewall grille used for air distribution was assumed to be a 75% free area air diffuser and 83 percent of the lighting energy was assumed to transmit downward into the room by convection and radiation. The boundary conditions for the velocity and turbulence properties included zero gradients in the exit plane and logarithmic wall functions to describe the near-wall or solid surface regions. All surfaces were assumed to be adiabatic except a portion of the floor and the ceiling around the room center and the top face of the concentrated load, where constant heat input rates were prescribed. Heat was supplied at a rate of 88.3 W/m^2 from the uniform load at the center of room floor, and at 3279 W/m^2 from the concentrated load in the vicinity of wall opposite to the inlet and at 26.7 W/m^2 from the fluorescent lights at the center of the ceiling. The heat inputs into the flow domain were assumed to be transmitted to the surrounding fluid cells immediately adjacent to the heated surfaces by adding corresponding heat source terms in the energy equation. As illustrated in Table 1, the inlet temperatures for six air inflow rates varying from 10.97 to 91.44 m^3/h-m^2 were respectively 17.3, 10.4, 5.2, 3.5, 2.6 and 2.1 °C lower than the average temperature of the room of 23.3 °C. The calculations of air velocity and temperature distributions for three-dimensional turbulent buoyant flows in a ventilated room were performed using the Cyber 205 supercomputer at the National Institute of Standards and Technology.

3 Calculated Results

Figures 1 to 6 show the calculated velocity distribution in the vertical center plane of the test room for the six different air inflow rates. As shown in Figure 1, the cold air coming from the inlet travelled down towards the floor due to the downward directed buoyancy force. A portion of flows circulated around the lower left corner of the room and exited through the return air grille. The remaining portions proceeded along the floor surface, turned upward after impinging onto the concentrated load, and after being accelerated by merging with the hot gas stream rising from the concentrated load, spread radially along the ceiling and entrained into the main flows from the inlet. Two recirculating zone were observed, one situated in the top right corner of the room and the other one near the floor in the vicinity of the concentrated load. The experimental air distribution patterns on the vertical center plane of the room obtained with smoke filaments for different flow rates [3,4] are given in Figure 7 for comparison with the predictions. As shown in Figures 1 and 7.a, the predicted general flow structure agrees quite well with the corresponding experimental observations. In Figure 2, the inflows following the ceiling spread radially toward the floor and the wall opposite to the entrance because of increased inlet velocity and decreased downward directed buoyancy effects. The flows are then curved along the wall and floor, and entrained into the jet stream or depart from the test room. It can be seen that a secondary recirculation is created in the vicinity of the ceiling and the concentrated heat source. It is interesting to note that the recirculation in this case has moved toward the ceiling in comparison to Figure 1 where the recirculation is along the floor. There is good agreement between prediction and experimental observations on flow patterns by comparison of Figures 2 and 7.b.

Figures 3 through 6 show a turbulent buoyant wall jet issuing from the inlet grille, spreading along the ceiling and turning downward and horizontally toward the outlet after impinging onto the opposite wall. A recirculating flow structure appeared in the whole flow domain with its center located near the concentrated load. The predicted flow patterns shown in Figures 3 to 6 are generally consistent with the corresponding experimental observations illustrated in Figure 7. Some examples of calculated isotherms in the middle section of the vented room are shown in Figures 8 through 10 where air supply rates per unit floor area are 18.29, 54.86 and 73.15 $m^3/h\text{-}m^2$, respectively. The temperature field is generally dependent upon the inlet air velocity, the temperature difference between the supply air and the room air, and the distribution and output rate of the heat sources. As shown in Figure 8, the air temperature increases with increasing distance away from the inlet grille due to continuous entrainment of warm air into the cold jet stream discharging from the inlet and flowing toward the floor. The air temperature exhibits a sharp gradient close to the heat source and its distribution generally agrees with the corresponding flow field illustrated in Figure 1. As shown in Figures 9 and 10, the isothermal lines in the upper portion of the room are nearly horizontal. These diminished temperature gradients and increased thermal stratification in the upper region are attributed to greater inlet velocities and better mixing of the cold supply air with warm room air.

The Air Diffusion Performance Index (ADPI) is commonly used to specify the performance of an air diffuser system, and is defined as the percentage of the locations in the occupied zone that meet acceptable limits of effective draft temperatures between - 1.7 °C and +1.1 °C, and local air velocity of less than 0.35 m/s [11]. The effective draft temperature, ϕ, can be calculated from the equation below:

$$\phi = (T_x - T_c) - 8.0(v_x - 0.15) \qquad (6)$$

where T_x is the local air temperature, in °C, T_c is the room average temperature, in °C and v_x is the local air velocity, in m/s.

The air diffusion performance indexes for the sidewall grille are calculated for different flow rates of supply air and listed in Table 2 along with the corresponding experimentally determined values. The ADPI calculations were based on predicted air temperatures and velocities at 96 locations, which were uniformly distributed throughout the occupied space in the one-half portion of the flow domain. The occupied zone was situated at 0.28 m from the wall of the inlet, 0.31 m from side walls, 0.79 m from the wall opposite to the inlet, and 0.17 m from the floor extending up to 1.87 m above the floor.

The predicted ADPI and drafty percentage values are generally in good agreement with the experimental ADPI and drafty percentage values. It can be noted that the experimental values were derived based on 216 measurement locations distributed evenly in a room space situated 0.92 m from the wall opposite to the inlet, 0.31 m from side walls and the wall of air inlet, 0.10 m from the floor, and 0.81 m from the ceiling or 1.93 m above the floor. At the highest two air inflow rates, there are slight discrepancies between the predicted and experimental ADPI results. This may be attributed to over-predicting the spread of the air wall jet after impinging onto the opposite wall and deflecting and reversing direction of flows as local air velocities decreased rapidly as shown in Figures 5 and 6. With the exclusion of the two highest air inflow rates, the predicted ADPI values are found to agree within 8% of the the corresponding experimental values. There are significant inconsistencies between the predicted and experimental results on the percentages of stagnant cold spots in the occupied zone. The use of lower values for temperature differential between the room air and the inlet air in calculations, for instance, 17.2 °C versus 19.4 °C [1], which was actually used to make up the 63.05 W/m^2 heating load for the test with a flow rate of 10.97 m^3/h-m^2, undoubtedly contribute to a part of this discrepancy. It was also noted that at higher flow rates, the results of the simulation were greatly influenced by the assumed inlet flow velocity even though the volumetric flow rate remained constant (that is, by increasing or decreasing the assumed effective area of the grille).

As illustrated in Table 2, the predicted ADPI values have a maximum at an air inflow rate of 18.29 m^3/h-m^2. At low rates of air supply, the jet of cool air fell downward due to strong buoyancy effect and did not fill the room. Under these conditions, there were thus numerous locations within the room at which the local temperatures were far below and above the control temperature causing the effective draft temperature to be outside the comfort limits and therefore leading to low ADPI values. With an increase in the supply of air, the ADPI values were increased to a maximum because of better mixing occurring within the room. However, a further increase in the volume of air supply resulted in a decrease in ADPI value since the number of locations with local air velocities greater than the 0.35 m/s limit was increased. The contour lines of constant draft temperature in a vertical plane separated by a distance of 0.27m from the plane of symmetry are shown in Figures 11 to 13, where air inflow rates per unit floor area are 18.29, 54.86 and 73.15 m^3/h-m^2, respectively. The distribution of effective draft temperatures can provide an indication of the level of human comfort in a local area. For the range of inflow rates employed to obtain these figures, the total size of the areas bounded by the contour lines of effective draft temeratures between -1.7°C and +1.1°C decreases with an increase in air supply rate. These findings are in good agreement with the measured and predicted Air Diffusion Performance Index values illustrated in Table 2.

4. Conclusions

Prediction of buoyancy-affected air flows emerging from an air diffuser in a ventilated room has been demonstrated over a wide range of air supply rates with constant heating loads using the numerical technique presented in this paper. The three-dimensional distributions of air velocity and temperature in an air conditioned room are calculated, and the calculated velocity distributions are generally in reasonably good agreement with experimental observations obtained with smoke filaments.

The Air Diffusion Performance Indexes (ADPI) for a sidewall grille are calculated for six air flow rates and the calculated results are compared with the corresponding published experimental values. Good agreement is obtained for flow rates ranging between 10.97 and 54.86 $m^3/h\text{-}m^2$ of floor area, and a fair agreement is found for flow rates greater than 73.15 $m^3/h\text{-}m^2$ which is probably due to use of smaller values for the heating loads and temperature differential between the room air and the inlet air in the numerical simulations compared to the experimental values. The ADPI value is found to be a function of air inflow rate, effective area of the air diffuser and room heating load as would be expected. The distribution pattern of effective draft temperatures in the flow domain reflects the profile of the local occupant's comfort level and can be used as a measure of the ADPI for a ventilated space. The procedure for calculating three velocity components and temperature in a ventilated room involves the solution of three-dimensional transient equations for conservation of mass, momentum, energy, and turbulence kinetic energy and its dissipation rate. The calculation procedure is practically useful in the design of building ventilation systems and prediction of various air-conditioned room environments.

5 References

1. Miller, P. L. and R. G. Nevins, 'An Analysis of the Performance of Room Air Distribution Systems; ASHRAE Transactions, 78, Part I, 191-198, (1972).
2. Miller, P. L., 'Room Air Distribution Performance of Four Selected Outlets', ASHRAE Transactions, 77, Part II, 194-204, (1971).
3. Miller, P. L. and R. T. Nash, 'A Further Analysis of Room Air Distribution Performance; ASHRAE Transactions, 77, Part II, 205-212, (1971).
4. Nevins, R. G., 'Air Diffusion Dynamics--Theory, Design and Application', Business News Publishing Co., Birmingham, Michigan, 1976.
5. Hart, G. H. and D. Int-Hout, 'Thermal Performance of a Continuous Linear Air Diffuser in the Perimeter Zone of an Office Environment', ASHRAE Transactions, 86, Part 2, 107-124, (1980).
6. Yamazaki, K., M. Komatsu and M. Otsubo, 'Application of Numerical Simulation for Residential Room Air Conditioning', ASHRAE Transactions, 93, Part 1, 210-225, (1987).
7. Chen, Qingyan, J. van der Kooi and A. Meyers, 'Measurements and Computations of Ventilation Efficiency and Temperature Efficiency in a Ventilated Room', Energy and Buildings, 12, 85-99, (1988)
8. Kurabuchi, T., 'Numerical Calculation Method of Indoor Air Flow by Means of k-E Turbulence Model, NISTIR Report (In Process).

9. Kurabuchi, T. and T. Kusuda, 'Numerical Prediction for Indoor Air Movement', ASHRAE Journal, December 1987, pp 26-30.

10. Harlow, F. H. and J. E. Welch, 'Numerical Calculation of Time Dependent Viscous Incompressible Flow of Fluid with Free Surface', Physics of Fluids, 8, 2182-2189 (1965).

11. American Society of Heating, Refrigerating and Air-Conditioning Engineers, 'ASHRAE Handbook - 1985 Fundamentals', Atlanta, GA, 1985.

Table 1. The Numerical Values of Temperature Difference between the Room Air and the Supply Air and Nondimensional Parameters Used in Numerical Calculations

Parameters Used in Numerical Simulations				
Inlet Flow Rate ($m^3/h\text{-}m^2$)	Inlet Velocity (m/s)	Temperature Difference (°C)	Reynolds Number	Archimedes Number
10.97	0.975	17.26	38860	0.365920
18.29	1.626	10.36	64430	0.079040
36.58	3.251	5.180	128860	0.009879
54.86	4.877	3.452	193290	0.002927
73.15	6.502	2.589	257710	0.001235
91.44	8.128	2.071	322150	0.000632

Table 2. Calculated ADPI Values for Different Flow Rates of Air Supply and the Corresponding Experimentally Determined Values

Inflow ($m^3/h\text{-}m^2$)	ADPI (%)	V > 0.35 m/s Drafty (%)	T > -2.8 °C φ<-1.7 °C Stagnant Cold (%)	T < 2.8 °C φ > 1.1 °C Stagnant Hot (%)
10.97	67	0.0	2.1	31.3
	(68)	(2.3)	(4.2)	(23.6)
18.29	83	2.1	12.5	4.2
	(79)	(3.7)	(6.9)	(10.2)
36.58	79	17.7	14.6	2.1
	(82)	(5.1)	(0.5)	(12.0)
54.86	68	30.2	30.2	2.1
	(74)	(25.9)	(0.5)	(0.0)
73.15	47	53.1	51.0	0.0
	(31)	(68.1)	(0.9)	(0.0)
91.44	38	61.5	62.5	0.0
	(20)	(79.2)	(0.5)	(0.0)

Note: The values in parentheses are the experimentally determined values.

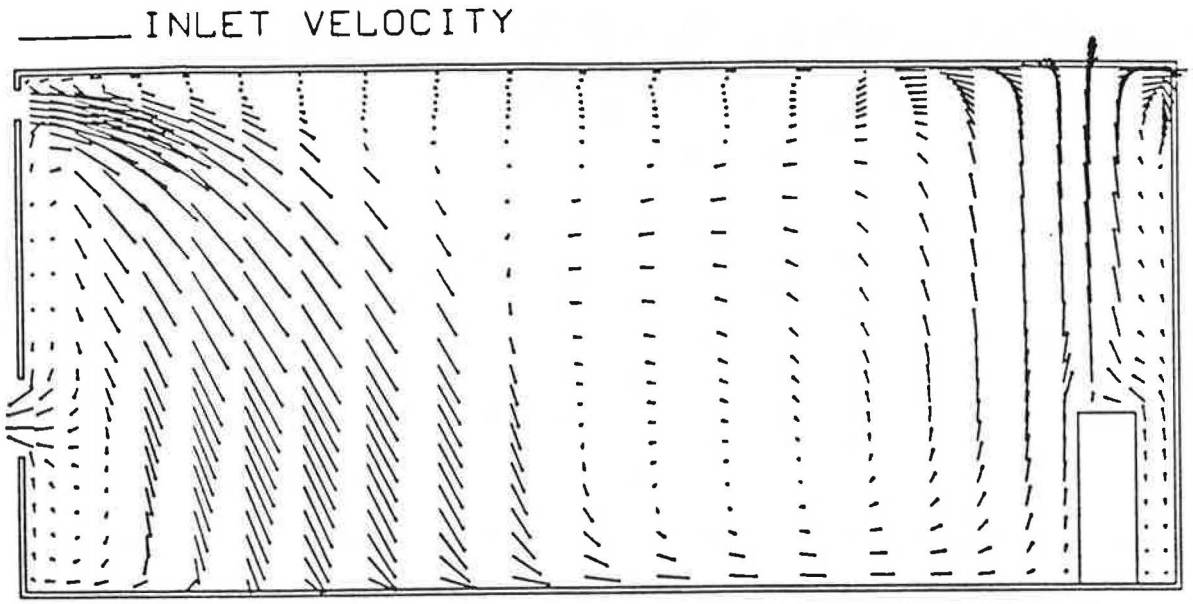

Figure 1. Distribution of Calculated Velocity Vectors in the Center Plane for Inflow Rate of 10.97 $m^3/h\text{-}m^2$

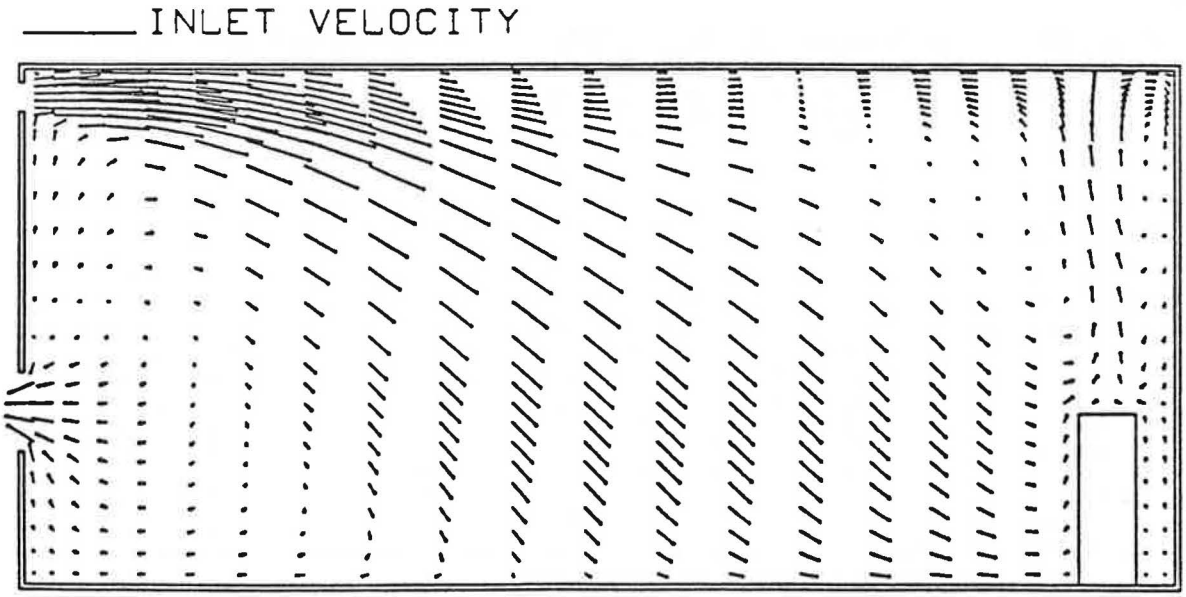

Figure 2. Distribution of Calculated Velocity Vectors in the Center Plane for Inflow Rate of 18.29 $m^3/h\text{-}m^2$

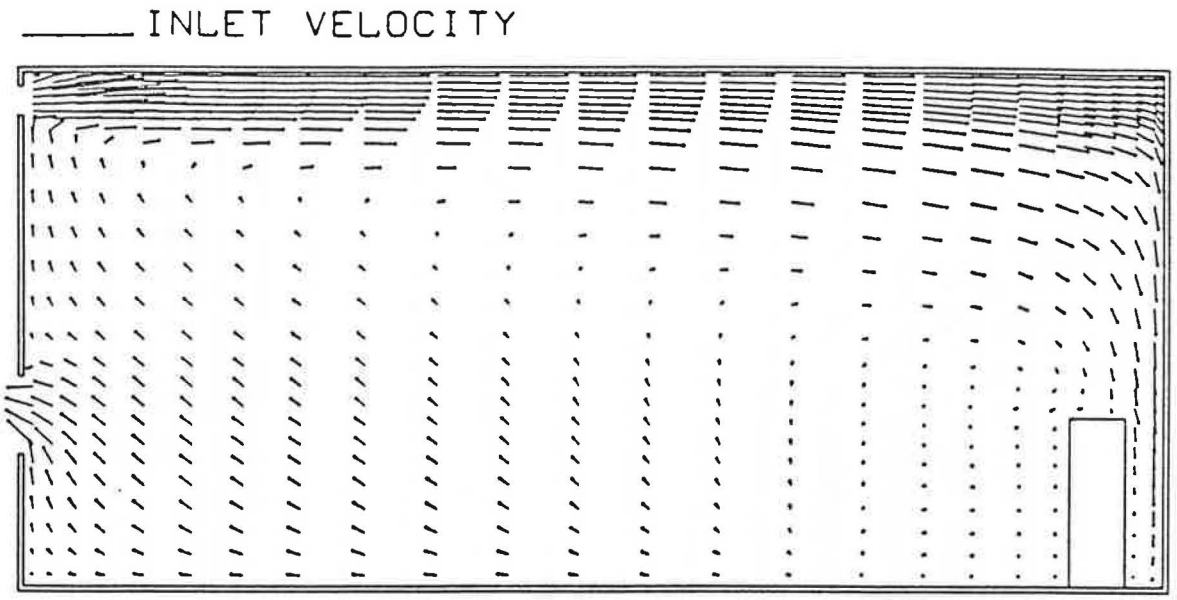

Figure 3. Distribution of Calculated Velocity Vectors in the Center Plane for Inflow Rate of 36.58 $m^3/h\text{-}m^2$

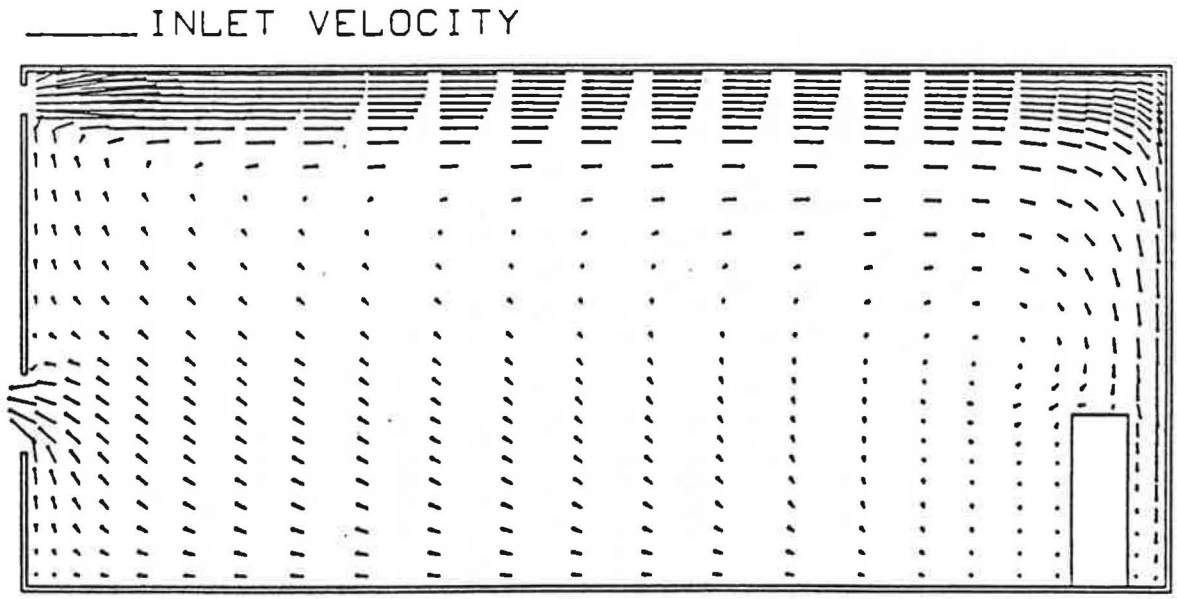

Figure 4. Distribution of Calculated Velocity Vectors in the Center Plane for Inflow Rate of 54.86 $m^3/h\text{-}m^2$

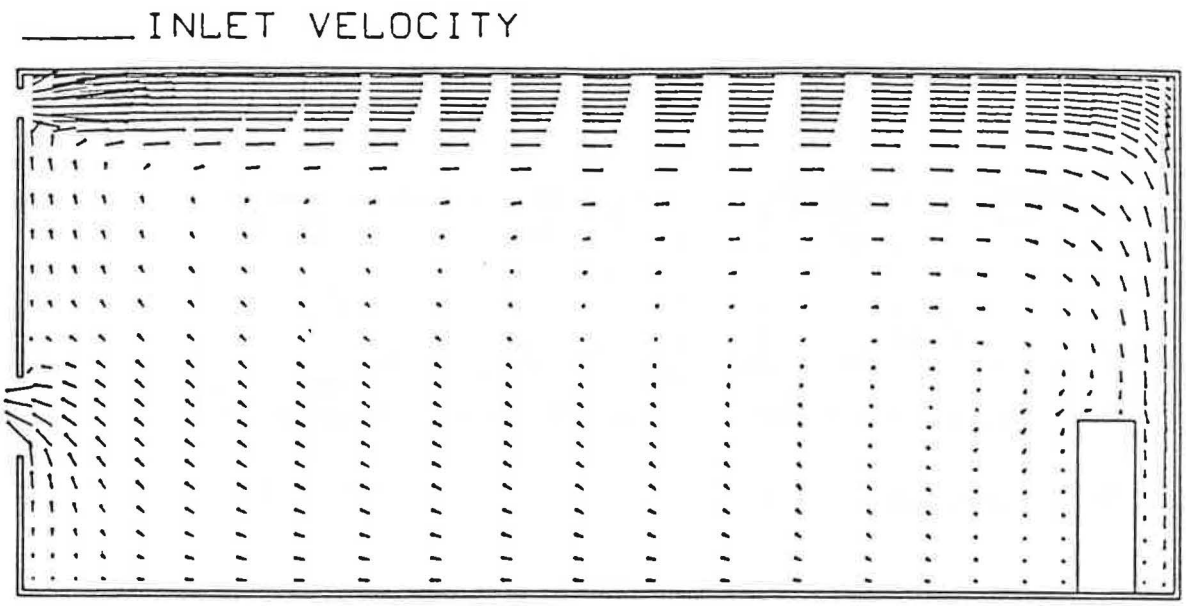

Figure 5. Distribution of Calculated Velocity Vectors in the Center Plane for Inflow Rate of 73.15 $m^3/h\text{-}m^2$

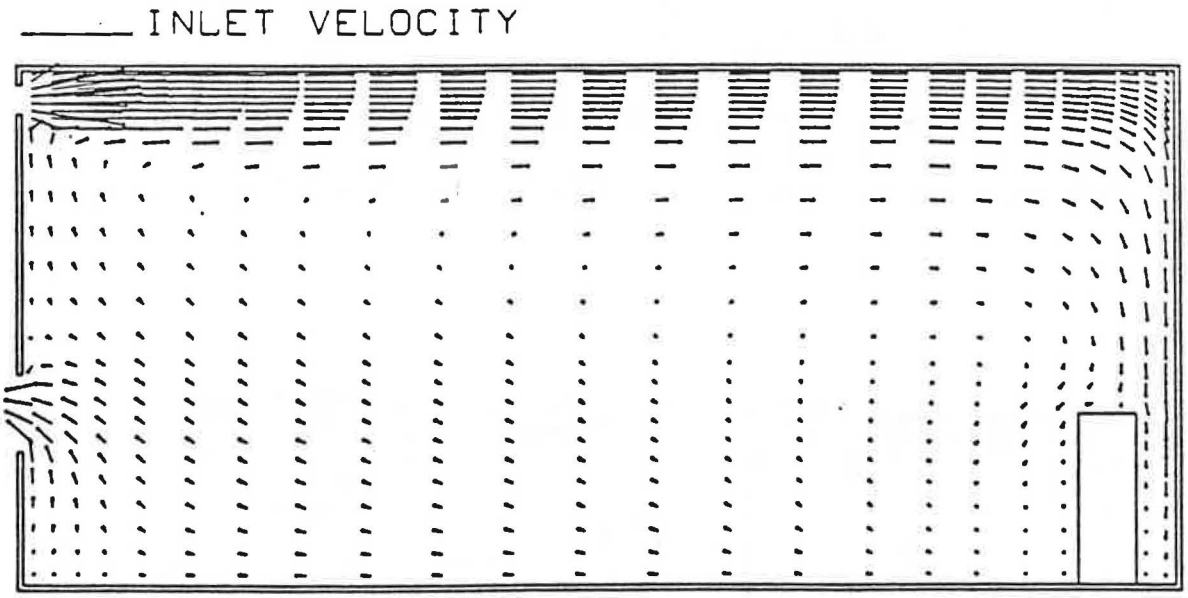

Figure 6. Distribution of Calculated Velocity Vectors in the Center Plane for Inflow Rate of 91.44 $m^3/h\text{-}m^2$

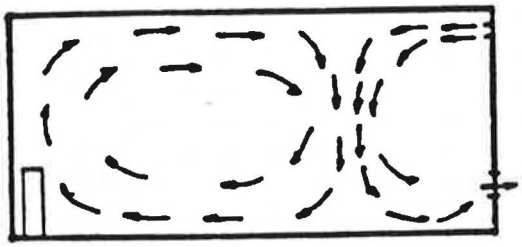

a. Inflow rate = 10.97 $m^3/h\text{-}m^2$

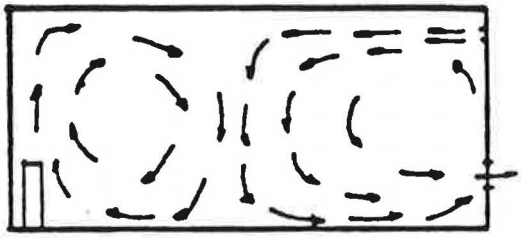

b. Inflow rate = 18.29 $m^3/h\text{-}m^2$

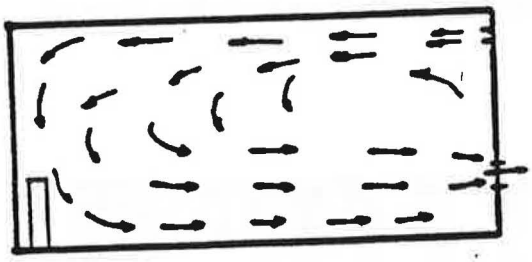

c. Inflow rate = 36.58 $m^3/h\text{-}m^2$

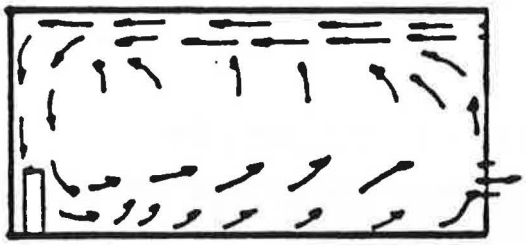

d. Inflow rate = 54.86 $m^3/h\text{-}m^2$

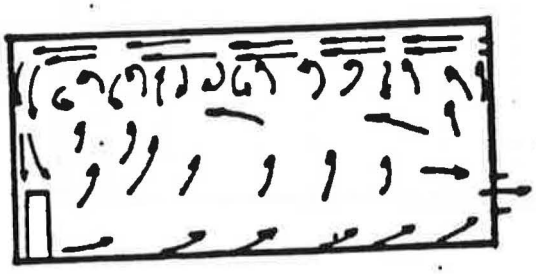

e. Inflow rate = 73.15 $m^3/h\text{-}m^2$

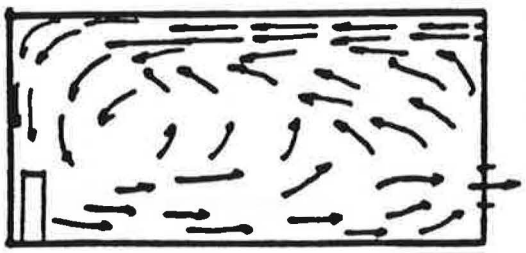

f. Inflow rate = 91.44 $m^3/h\text{-}m^2$

Figure 7. Measured Air Flow Patterns for Different Air Flow Rates

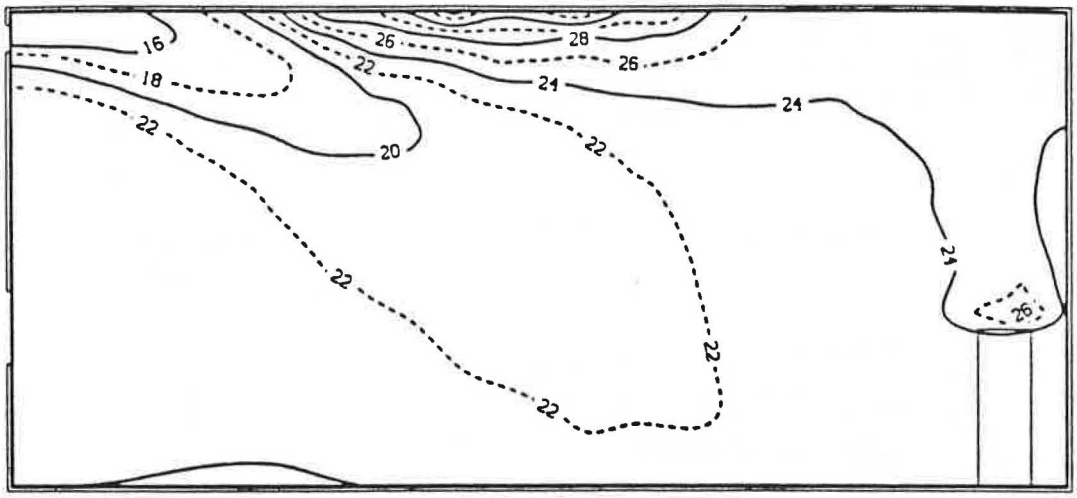

Figure 8. Calculated Isotherms in the Center Plane for Inflow Rate of 18.29 $m^3/h\text{-}m^2$

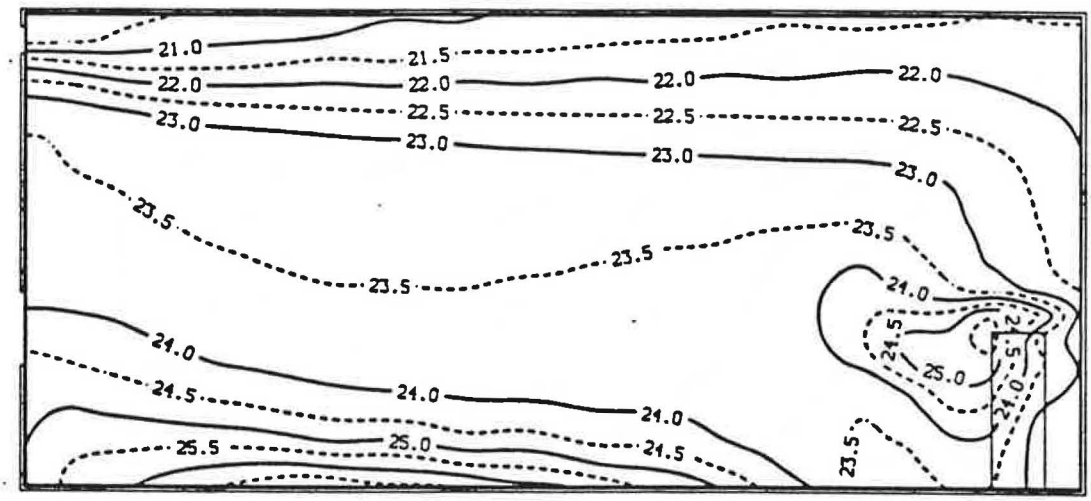

Figure 9. Calculated Isotherms in the Center Plane for Inflow Rate of 54.86 $m^3/h\text{-}m^2$

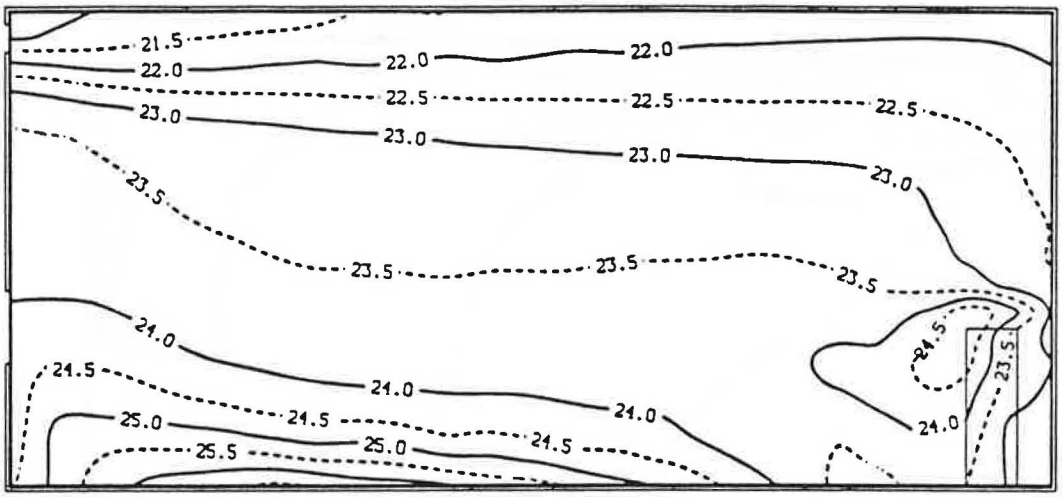

Figure 10. Calculated Isotherms in the Center Plane for Inflow Rate of 73.15 $m^3/h\text{-}m^2$

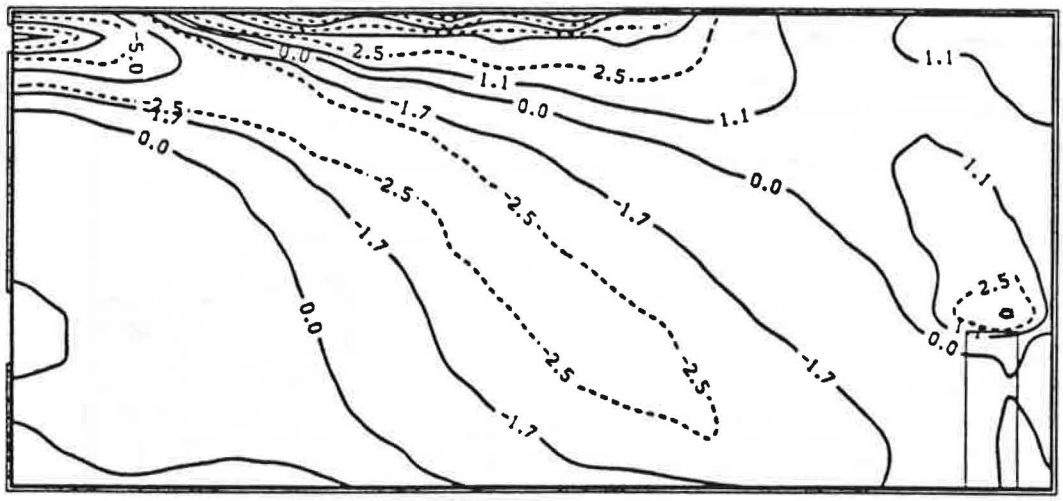

Figure 11. Contour Lines of Effective Draft Temperature in a Vertical Plane for Inflow Rate of 18.29 $m^3/h\text{-}m^2$

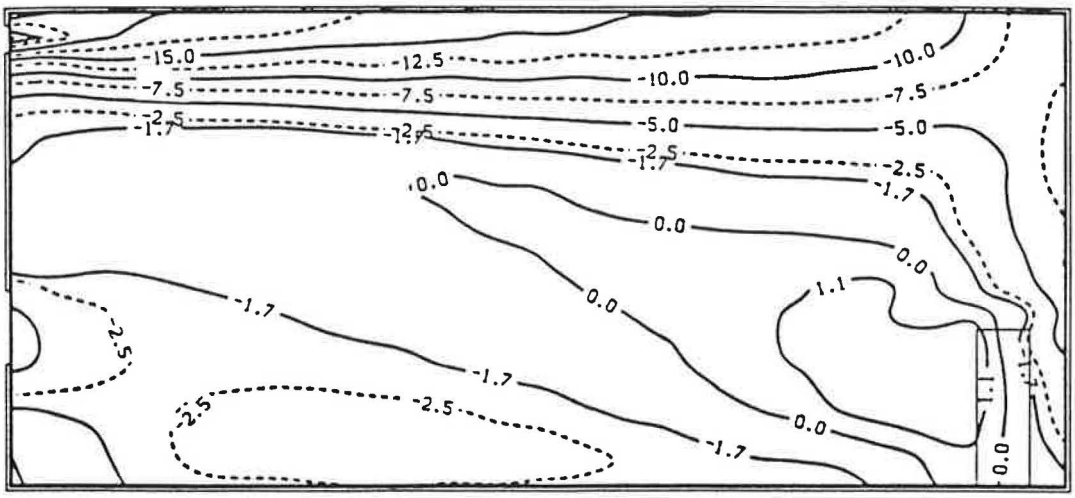

Figure 12. Contour Lines of Effective Draft Temperature in a Vertical Plane for Inflow Rate of 54.86 $m^3/h\text{-}m^2$

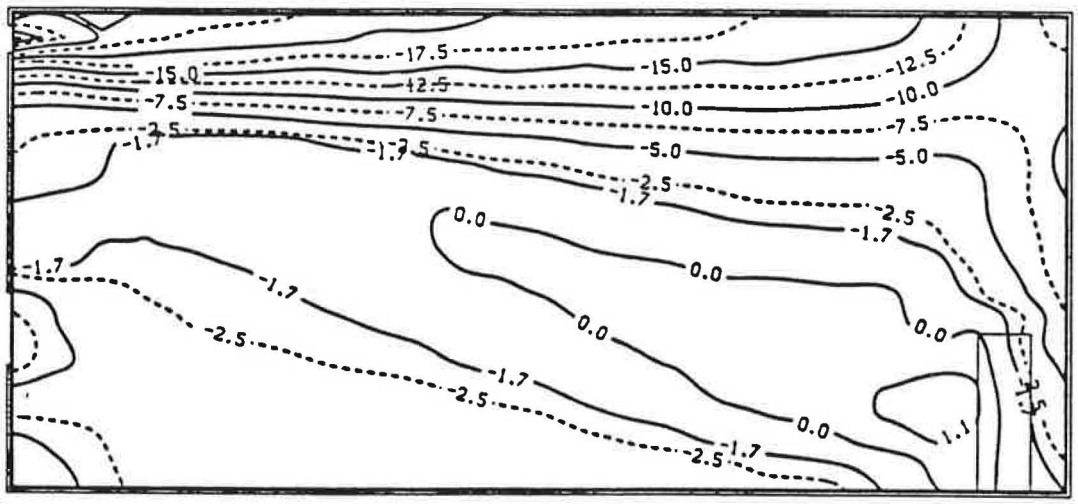

Figure 13. Contour Lines of Effective Draft Temperature in a Vertical Plane for Inflow Rate of 73.15 $m^3/h\text{-}m^2$